

# Nonlinear shock acceleration and $\gamma$ -ray emission from Tycho and Kepler

G. Morlino\* and D. Caprioli†

\*INAF - Osservatorio Astrofisico di Arcetri, L.go E. Fermi 5, I - 50125 Firenze, Italia

†Department of Astrophysical Sciences, Princeton University, Princeton, NJ 08544, USA

**Abstract.** We apply the non-linear diffusive shock acceleration theory in order to describe the properties of two supernova remnants, SN 1572 (Tycho) and SN 1604 (Kepler). By analyzing the multi-wavelength spectra, we infer that both Tycho's and Kepler's forward shocks (FS) are accelerating protons up to  $\sim 500$  TeV, channeling into cosmic rays more than 10 per cent of their kinetic energy. We find that the streaming instability induced by cosmic rays is consistent with the X-ray morphology of the remnants, indicating a very efficient magnetic field amplification (up to  $\sim 300\mu\text{G}$ ). In the case of Tycho we explain the  $\gamma$ -ray spectrum from the GeV up to the TeV band as due to pion decay produced in nuclear collisions by accelerated nuclei scattering against the background gas. On the other hand, due to the larger distance, the  $\gamma$ -ray emission from Kepler is not detected, being below the sensitivity of the present detectors, but it should be detectable by CTA.

**Keywords:** Shock acceleration; cosmic rays; supernova remnants; gamma rays

**PACS:** 98.38.Mz; 95.85.Nv; 95.85.Pw; 98.70.Sa

## INTRODUCTION

Modelling particle acceleration at SNRs is one of the main goal to explain the origin of Galactic cosmic rays (CRs) in the context of the so-called *supernova paradigm* [see e.g. 1]. This paradigm requires that SNRs are able to accelerate nuclei up to energies as high as a few times  $10^6$  GeV, converting a fraction  $\sim 10\%$  of the SNR kinetic energy into CRs. There is an increasing amount of evidence that shocks in young SNRs can indeed reach the required efficiency. Unfortunately, all these evidence are indirect and when considered individually can be also explained by other mechanisms that do not require efficient acceleration. A clear example of such an ambiguous situation is represented by  $\gamma$ -ray emission. In the last few years several SNRs have been detected both in the GeV and in the TeV band but, in spite of this increasing amount of data, the question whether this emission is due to hadronic (through the decay of neutral pions produced in nuclear interactions between accelerated nuclei and the background plasma) or leptonic processes (due to inverse Compton and/or bremsstrahlung) is still debated [see e.g. 2, for a general discussion on this topic]. A possible way to discriminate between the *leptonic* (i.e. inefficient) and the *hadronic* (i.e. efficient) scenario is studying the effects that particle acceleration produces at all observable wavelengths, rather than focus the attention only on the  $\gamma$ -ray emission, simultaneously using multiple set of data to constrain the model.

Here we apply the non-linear diffusive shock acceleration (NLDSA) theory in order to explain the non-thermal emission and morphological properties of two similar SNRs, namely Tycho and Kepler. Tycho, in particular, has been recently detected in  $\gamma$ -rays by

Fermi-LAT [3] and VERITAS [4], and can be considered one of the most promising object where to test the shock acceleration theory and hence the CR–SNR connection. We presented a detailed model applied to Tycho in [5]. Kepler, on the other hand, has not been detected in  $\gamma$ -ray band, yet, but it is very similar to Tycho in many respects, and we show that the predicted  $\gamma$ -ray spectrum should be detectable by CTA.

## COUPLING PARTICLE ACCELERATION WITH REMNANT EVOLUTION

Both Tycho and Kepler have been established to be remnants of a type Ia SN, Tycho thanks to observation of the scattered-light echo [6] while Kepler based on the O/Fe ratio observed in the X-ray spectrum [7]. They have similar ages and similar values for the radio spectral index, i.e. 0.65 and 0.64, respectively. Interestingly also the ratio of power emitted at 10 keV and at 1 GHz, i.e.  $\nu F_\nu(@10\text{keV})/\nu F_\nu(@1\text{GHz})$ , is very similar, being 56.9 for Tycho and 52.9 for Kepler. Finally, both remnants present very thin filaments in non-thermal X-ray emission.

In order to make the model as simple as possible, in both cases we assume that the remnants expand into an uniform circumstellar medium (CSM) with proton number density  $n_0$  (which we leave as a free parameter) and temperature  $T_0 = 10^4$  K. We model the remnant evolution by following the analytic prescriptions given by [8] for Type Ia SNe, assuming a SN explosion energy  $E_{SN} = 10^{51}$  erg and one solar mass in the ejecta, whose structure function is taken as  $\propto (v/v_{ej})^{-7}$ . The radial structure of density and temperature profiles is then calculated by assuming that the shocked CSM is roughly in pressure equilibrium.

On top of this SNR evolution, the spectrum of accelerated particles is calculated according to the semi-analytic kinetic formalism put forward in [9] and references therein, which solves self-consistently the equations for conservation of mass, momentum and energy along with the diffusion-convection equation describing the transport of non-thermal particles for quasi-parallel, non-relativistic shocks. The injection is regulated by a free parameter,  $\xi_{inj}$ , in such a way that all particles from the thermal plasma with momentum  $p > \xi_{inj} p_{th,2}$ , with  $p_{th,2}$  the typical thermal momentum downstream, start the acceleration process.

A crucial role in our model is played by the magnetic field amplification induced by the super-Alfvénic streaming of relativistic particles upstream of the shock. We model this magnetic amplification as in [10]. The large magnetic fields predicted by the resonant amplification have two main consequences: 1) the magnetic pressure upstream becomes comparable to, or even larger than, the thermal plasma pressure and, reducing the compressibility of the plasma, affects the shock compression factor. 2) When the magnetic field is amplified the velocity of the scattering centers, which is generally neglected with respect to the shock speed, may be significantly enhanced [10]. When this occurs, the total compression factor felt by accelerated particles may be appreciably reduced and, in turn, the spectra of accelerated particles may be considerably softer. We explicitly include these effects assuming that the scattering centers moves with a speed equal to the Alfvén speed in the amplified magnetic field. Once the magnetic field structure is known, we can compute the spectrum of accelerated electrons at the shock, which

is assumed to be proportional to the proton spectrum  $f_e(p) = K_{ep}f_p(p)$ , up to a maximum momentum  $p_{e,\max}$  determined by the synchrotron losses in the amplified magnetic field, where the spectrum presents a squared exponential cut-off  $\propto \exp[-(p/p_{e,\max})^2]$ . The evolution of the electron and proton spectrum downstream of the shock is computed taking into account adiabatic losses for protons and adiabatic and synchrotron losses for electrons.

**RESULTS.** We consider the following radiative processes: 1) synchrotron emission of relativistic electrons; 2) thermal and non-thermal electron bremsstrahlung; 3) inverse Compton scattering (ICS) of electrons on CMB radiation, local IR dust emission and Galactic IR+optical light; 4) emission due to the decay of  $\pi^0$  produced in hadronic collisions. Because the explosion energy and the mass of the ejecta are fixed *a priori*, in order to fit the observed spectra and the remnant angular size we can only vary three parameters: the number density of the upstream medium,  $n_0$ , the injection efficiency of protons,  $\xi_{\text{inj}}$ , and the electron to proton normalization,  $K_{ep}$ .

In Fig. 1 we show our best fit of the photon spectrum produced by the superposition of all the radiative processes outlined above, comparing it with the existing data. The overall agreement is quite good. Quite interestingly, for both Tycho and Kepler our best-fitting returns  $n_0 = 0.3 \text{ cm}^{-3}$  and  $\xi_{\text{inj}} = 3.7$  which implies that the total amount of kinetic energy channeled into CRs is  $\simeq 12\%$ . The inferred values for the circumstellar medium implies that Tycho and Kepler have a distance of 3.3 and 7.4 kpc from the Sun.

Synchrotron radiation fits well the observed X-ray emission assuming an electron to proton ratio  $K_{ep} = 1.6 \times 10^{-3}$  for Tycho and  $2.8 \times 10^{-3}$  for Kepler. The projected X-ray emission profile is shown in Fig.2, where it is compared with available Chandra data. In the case of Tycho the predicted profile shows a very good agreement with the data while for Kepler the model overpredicts the emission in the inner part of the rim. This could be due to a deviation of the shock geometry from the perfectly spherical symmetry assumed in our model. The sharp decrease of the emission behind the FS is due to the rapid synchrotron losses of the electrons in a magnetic field as large as  $\sim 300 \mu\text{G}$ .

In the  $\gamma$ -ray band the decay of  $\pi^0$  produced in hadronic collision is the dominant process. In particular, we predict a slope for accelerated protons  $\propto E^{-2.2}$ . In the case of Tycho this slope well accounts for Fermi-LAT and VERITAS data within the experimental errors. The predicted proton spectrum shows a cut-off around  $p_{\max} = 470 \text{ TeV}/c$ .

ICS of relativistic electrons cannot explain the observed  $\gamma$ -ray emission for two different reasons. First, the strong magnetic field produced by the CR-induced streaming instability forces the number density of relativistic electrons to be too small to explain the  $\gamma$ -ray emission as due to ICS on the ambient photons. Second, even if we arbitrarily reduced the magnetic field strength, enhancing at the same time the electron number density in order to fit the TeV  $\gamma$ -rays with ICS emission, we could not account for the GeV  $\gamma$ -rays because both the spectral slope and the flux would be incompatible with the Fermi-LAT data. Also non-thermal electron bremsstrahlung has to be ruled out, because it provides a flux two order of magnitudes lower than the Fermi-LAT detection, and cannot be arbitrarily enhanced without over-predicting both the TeV and the X-ray emission. Kepler, due to its larger distance, it is fainter than Tycho and therefore not detected in the  $\gamma$ -ray band by the current generation of telescopes. However, the predicted TeV flux should be observable by the Cerenkov Telescope Array.

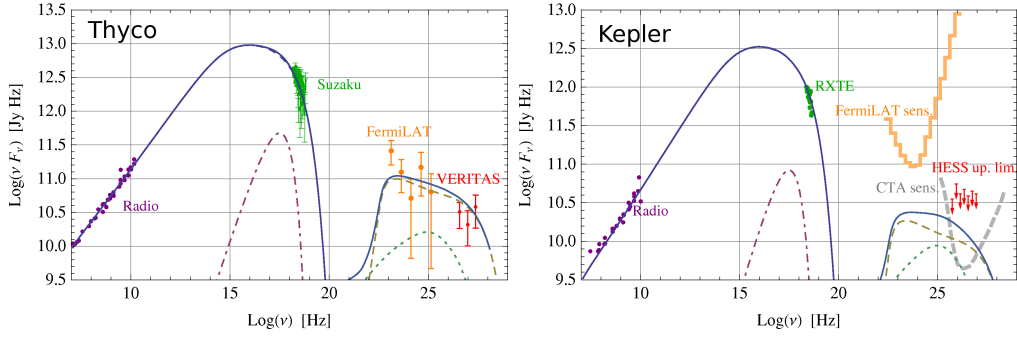


**FIGURE 1.** Spatially integrated spectral energy distribution of Tycho (left panel) and Kepler (right panel). The curves show synchrotron emission (thin dashed), thermal electron bremsstrahlung (dot-dashed),  $\pi^0$  decay (thick dashed) and ICS (dotted) as calculated within our model. The total emission is showed by the solid curve. The experimental data for Tycho are, respectively: radio from [11]; X-rays from Suzaku (courtesy of Toru Tamagawa), GeV  $\gamma$ -rays from Fermi-LAT [3] and TeV  $\gamma$ -rays from VERITAS [4]. For Kepler: radio from [11] and X-rays from [12].

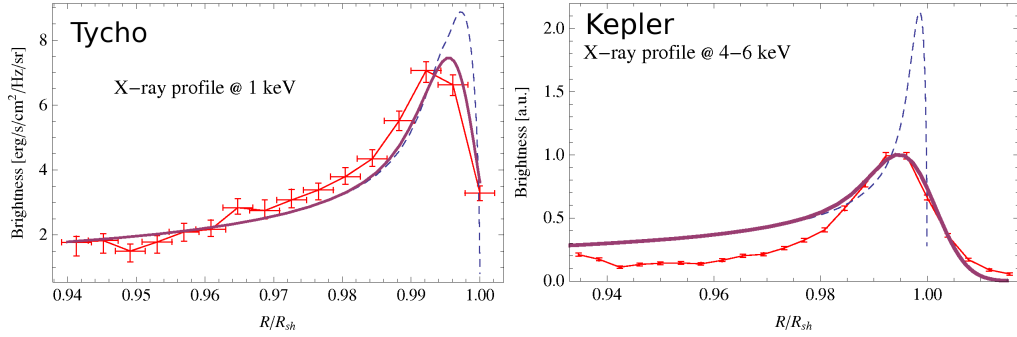


**FIGURE 2.** Projected X-ray emission at 1 keV for Tycho (left panel) and at 4-6 keV for Kepler (right panel) as a function of the distance from the shock position. The *Chandra* data points are from [13] (for Tycho) and from [14] (for Kepler). The dashed lines shows the projected radial profile of synchrotron emission while the solid lines are the same but convolved with the *Chandra* point spread function ( $\sim 0.5''$ ).

## REFERENCES

1. Drury, L. O'C, Aharonian, F., Völk, H. J., *A&A* **287**, 959- (1994)
2. Ellison, D. C., Patnaude, D. J., Slane, P., Blasi, P., Gabici, S., *ApJ* **661**, 879- (2007)
3. Giordano, F. et al., *ApJ* **744**, 2- (2012)
4. Acciari, V. A. et al., for the VERITAS collaboration, *ApJ* **730**, L20- (2011)
5. Morlino, G. & Carpioli, D., *A&A* **538**, 81- (2012)
6. Krause, O. et al., *Nature* **456**, 617- (2008)
7. Reynolds, S. P., Borkowski, K. J., Hwang, U., et al., *ApJ* **668**, L135- (2007)
8. Truelove, J. K. and Mc Kee, C. F., *Apj Supplement Series* **120**, 299- (1999)
9. Caprioli, D., Amato, E., P. Blasi, *APh* **33**, 307- (2010)
10. Caprioli, D., *JCAP* **7**, 38- (2012)
11. Reynolds, S. P., & Ellison, D. C., *ApJ* **339**, L75- (1992)
12. Allen, G. E., Gotthelf, E. V., Petre, R., *Proceedings of the 26th ICRC* **3**, 480- (1999)
13. Cassam-Chenaï, G., Hughes, J. P., Ballet, J., Decourchelle, A., *ApJ* **665**, 315- (2007)
14. Vink, J., *ApJ* **689**, 231- (2008)